HHS Public Access

Author manuscript

Clin Cancer Res. Author manuscript; available in PMC 2021 July 15.

Published in final edited form as:

Clin Cancer Res. 2021 January 15; 27(2): 554–565. doi:10.1158/1078-0432.CCR-20-1422.

Altered Gemcitabine and Nab-paclitaxel Scheduling Improves Therapeutic Efficacy Compared to Standard Concurrent Treatment in Pre-clinical Models of Pancreatic Cancer

Adam R. Wolfe[^,1], **Ryan Robb**[^,1], **Ahmad Hegazi**[1], **Laith Abushahin**[3], **Linlin Yang**[1], **Duan-Liang Shyu**[1], **Jose G. Trevino**[2], **Zobeida Cruz-Monserrate**[3], **John Jacob**[1], **Kamalakannan Palanichamy**[1], **Arnab Chakravarti**[1], **Terence M. Williams**[1,*]

[1]Department of Radiation Oncology, The Ohio State University Wexner Medical Center, Arthur G. James Comprehensive Cancer Center and Richard J. Solove Research Institute, Columbus, OH 43210, USA.

[2]Department of Surgery, University of Florida College of Medicine, Gainesville, FL 32610, USA.

[3]Departement of Internal Medicine, Division of Gastroenterology, Hepatology, and Nutrition, The Ohio State University Wexner Medical Center, Columbus, OH 43210, USA.

Abstract

Background: Concurrent gemcitabine and *nab*-paclitaxel treatment is one of the preferred chemotherapy regimens for metastatic and locally-advanced pancreatic ductal adenocarcinoma (PDAC). Previous studies demonstrate that caveolin-1 (Cav-1) expression is critical for *nab*-paclitaxel uptake into tumors and correlates with response. Gemcitabine increases *nab*-paclitaxel uptake by increasing Cav-1 expression. Thus, we hypothesized that pre-treatment with gemcitabine would further enhance the sensitivity of PDAC to *nab*-paclitaxel by increasing Cav-1 expression and *nab*-paclitaxel uptake.

Methods: We investigated the sensitivity of different gemcitabine and *nab*-paclitaxel treatment regimens in a panel of PDAC cell lines and orthotopic xenograft models. The sensitivity of different treatment regimens was compared to the standard concurrent treatment.

[*]**Corresponding Author**: Terence M. Williams, Department of Radiation Oncology, The Ohio State University, 460 W. 12th Avenue, BRT/Room 492, Columbus, OH 43210, USA. Phone:(614) 366-2621. Fax: (614) 293-4044. terence.williams@osumc.edu.

[^]authors contributed equally to the work

Authors' Contributions

Conception and design: T.M. Williams

Development of methodology: R. Robb, A. Wolfe, K. Palanichamy, T.M. Williams

Acquisition of data (provided animals, acquired and managed patients, provided facilities, etc.): R. Robb, A. Wolfe, A. Hegazi, L. Yang, D-L Shyu, J. Jacob, K. Palanichamy

Analysis and interpretation of data (e.g., statistical analysis, biostatistics, computational analysis): R. Robb, A. Wolfe, K. Palanichamy, T.M. Williams

Writing, review, and/or revision of the manuscript: A. Wolfe, R. Robb, L. Abushahin, T.M. Williams

Administrative, technical, or material support (i.e., reporting or organizing data, constructing databases): T.M. Williams, J. Trevino, Z. Cruz-Monserrate, A. Chakravarti, L. Abushahin

Study supervision: T.M. Williams

Financial Disclosure Statements: All authors have no competing financial interests to disclose.

Conflict of Interest: None

Results: Pre-treatment with gemcitabine before *nab*-paclitaxel increased Cav-1 and albumin uptake and significantly decreased proliferation and clonogenicity compared to concurrent treatment, which correlated with increased levels of apoptosis. Cav-1 silencing reduced the uptake of albumin and therapeutic advantage observed when cells were pre-treated with gemcitabine prior to *nab*-paclitaxel. Additionally, we observed that pre-treatment with gemcitabine resulted in partial synchronization of cells in the G2/M phase at the time of *nab*-paclitaxel treatment, providing another mechanism for the benefit of altered scheduling. In heterotopic and orthotopic xenograft models, the altered schedule of gemcitabine prior to *nab*-paclitaxel significantly delayed tumor growth compared to concurrent delivery without added toxicity.

Conclusion: Pre-treatment with gemcitabine significantly increased *nab*-paclitaxel uptake and correlated with an increased treatment efficacy and survival benefit in preclinical models, compared to standard concurrent treatment. These results justify preclinical and clinical testing of this altered scheduling combination.

Keywords

gemcitabine; nab-paclitaxel; pancreatic cancer; scheduling; caveolin-1

INTRODUCTION:

In the U.S., there will be an estimated 56,770 new cases of pancreatic carcinoma and 45,750 estimated deaths in 2019 (1). The 5 year overall survival (OS) rate remains dismal at only 10%, and consequently pancreatic ductal adenocarcinoma (PDAC) is projected to become the 2nd leading cause of cancer-related death by 2030 (2). With curative surgery, 5 year survival rates approach 27% but distant failure rates remain high at 44% (3). Historically, gemcitabine was the chemotherapy of choice for both metastatic and resected PDAC based on clinical trial results which showed an improved OS benefit and greater response rates compared to observation or 5-fluoruracil (5-FU) chemotherapy in both the metastatic and adjuvant setting (4, 5). Recently, the combination regimens of either 5-FU/leucovorin with irinotecan and oxaliplatin (FOLFIRINOX), or gemcitabine and nanoparticle albumin-bound paclitaxel (NP, *nab*-paclitaxel or Abraxane®) are now standard of care in multiple settings based on phase III clinical trials showing superior outcomes with either of the combination chemotherapy regimens over gemcitabine alone (6–8). However, minimal attention is often paid to the effects of sequencing different combinations of chemotherapy agents before clinical testing.

Caveolin-1 (Cav-1) is the principal structural component of caveolae and is a key player in cellular endocytosis (12). PDAC has been shown to have high expression of Cav-1, and higher Cav-1 expression is associated with poor clinical outcomes, enhanced tumor progression, and resistance to gemcitabine in PDAC pre-clinical studies (13–15). Furthermore, knockdown of Cav-1 reduces PDAC uptake of albumin and NP, leading to reduced response to NP (16). For patients receiving gemcitabine and NP, the current standard of care is concurrent treatment of the drug combination on the same day. Interestingly, we observed that gemcitabine treatment of PDAC cells led to an increase in Cav-1 expression after 24–48 hours (13). We therefore hypothesized that pre-treatment with gemcitabine could be a strategy to increase NP uptake into PDAC cells through caveolae-

mediated endocytosis, and ultimately result in greater efficacy of the drug combination. Herein we provide evidence that gemcitabine treatment up to 48 hours prior to NP treatment increases the therapeutic efficacy of the combination, and represents a novel, simple and highly-translatable approach to potentially significantly improve outcomes for patients with PDAC.

MATERIALS AND METHODS:

Treatments, Reagents, Antibodies

Gemcitabine (Hospira; Lake Forest, IL) was dissolved in water. *Nab*-paclitaxel (Abraxane®, provided by Celgene; Summit, NJ) was dissolved in 0.9% saline. Trametinib (Selleckchem; Houston, TX) and RO-3306 (Millipore Sigma; St. Louis, MO) were dissolved in DMSO. RPMI 1640 media, Minimum Essential Media (MEM), McCoy's 5a media, penicillin (100 U/ml)-streptomycin (100 μg/ml), and 0.25% w/v trypsin/1 mM EDTA were purchased from Gibco Life Technologies (Grand Island, NY). Dulbecco's Modified Eagle Medium (DMEM) and phosphate-buffered saline (PBS) were purchased from GE Healthcare Bio-Sciences (Pittsburg, PA). Fetal Bovine Serum (FBS) and lyophilized powder Human Serum Albumin (HSA) was purchased from Millipore-Sigma (St. Louis, MO). Anti-cleaved caspase-8, cleaved caspase-7, cleaved caspase 3, cleaved PARP, human albumin, and GAPDH primary antibodies were purchased from Cell Signaling Technology (Danvers, MA). Caveolin-1 primary antibody (N-20) was purchased from Santa Cruz Biotechnology (Santa Cruz, CA). Anti-rabbit immunofluorescent secondary antibodies were purchased from LI-COR Biosciences (Lincoln, NE).

Cell Culture

AsPC-1, HPAF-II, MIA-PaCa-2, BxPC3, Capan-2, and CFPAC-1 cells were obtained from ATCC (Manassas, Virginia) and authenticated (via short tandem repeat profiling). FHs-74Int cells were also obtained directly from ATCC. Mouse PDAC cells derived from a pancreatic tumor of a *LSL-KRas*^{G12D}, *LSL-Trp53*$^{-/-}$, *PDX-1-CRE*, (KPC) genetically engineered mouse model of PDAC and transfected with enhanced firefly luciferase (KPC-Luc) as previously described were provided by Dr. Cruz-Monserrate (17, 18). Stable shRNA Cav-1 knockdown MIA-PaCa-2 cells were generated as described previously (16). Cells were maintained at 37°C in 5% CO_2 in RPMI 1640 media (AsPC-1), MEM (HPAF-II), DMEM (MIA-PaCa-2, G37, KPC-Luc), or ATCC Hybri-Care Medium 46-X (DMEM-like) + 30 ng/ml EGF (FHs 74Int) supplemented with 10% FBS and 1% penicillin/streptomycin. Cells were cultured for no more than 3 months continuously. Gemcitabine, *nab*-paclitaxel, trametinib, and RO-3306 were added to media with a vehicle final concentration of no more than 0.1%.

G37 PDX tumor-derived cell line generation

G37, a patient-derived xenograft (PDX) tumor model (a low Cav-1 expressing model obtained from Dr. Trevino) established from a surgically resected pancreatic adenocarcinoma patient, was passaged in the flanks of NOD-*scid* IL2Rgamma^{null} (NSG) mice using 2–3 mm^3 tumor fragments. G37 tumors were harvested 30–60 days post-implantation, and a portion (6 to 8 mm in diameter) of tumor was cut into fine tissue

particles. These were trypsinized at 37°C for 10 minutes, neutralized by DMEM containing 10% FBS, and then passed through 21G needles followed by 25G needle 3 times each, before transfer through 100μm cell strainers. The pass-through was transferred onto a fresh 10cm dish coated with 6–10 μg/cm^2 collagen (Millipore-Sigma; St. Louis, MO). This tumor cell mixture was cultured in DMEM containing 10% FBS and 10nM dexamethasone (Millipore-Sigma; St. Louis, MO) in 37°C incubators. Following 7–14 days of growth, G37 cells were passaged and sub-cultured for future use.

Cellular proliferation assay

alamarBlue® proliferation assay was performed according to the manufacturer's instructions (BioRad Antibodies, Oxford, UK). Briefly, cells were seeded in 96-well plates in 6 replicates at a density of 1,000–5,000 cells per well in 100 μL medium (Day 0). Between 48–72 hours after plating, alamarBlue® reagent was added and incubated at 37°C for 4–8 hours, and absorbance was measured at 570 and 600 nm.

Cell Proliferation using IncuCyte

Cells were seeded at 1,000–2,000 cells per well in 96-well plates. The next day, cells were treated according to schedule. Cell confluence as a measure of cell growth over time was monitored every 4 hours for up to 4 days using the IncuCyte ZOOM Live-Cell Imaging System (Essen Biosciences).

Colony forming assay

Cells were trypsinized to generate single cell suspensions. AsPC-1 (1,500 cells per plate), HPAF-II (1,500 cells per plate), G37 (3,000 cells per plate), and KPC-Luc (1,000 cells per plate) cells were seeded overnight onto 60 mm dishes. Plates were treated and allowed to grow until sufficiently large colonies were observed in the control plate (9–14 days after seeding). Colonies were fixed with Methanol/Acetic Acid, and stained with 1% crystal violet (Millipore-Sigma; St. Louis, MO). The numbers of colonies or colony forming units (CFU) containing at least 50 cells were counted using a dissecting microscope (Leica Microsystems, Inc. Buffalo Grove, IL).

Immunofluorescence

Cells were plated on coverslips and treated with or without gemcitabine. 2 hours prior to fixation cells were pulsed with 100 nM *nab*-paclitaxel or molar equivalent concentrations of human serum albumin (HSA). In order to remove membrane-bound albumin, two acid/salt washes were performed with 0.1M glycine and 0.1M NaCl, pH 3.02 on ice for 2 minutes each, followed by two washes with phosphate buffer saline (PBS) to remove membrane-bound albumin. Cells were then fixed with 2% paraformaldehyde for 15 minutes at room temperature, and washed with PBS 2 times for 5 minutes each. Cells were incubated in 1% Triton-x-100 for 10 min on ice to permeabilize, then washed twice with PBS prior to blocking with 3% bovine serum albumin in PBS overnight at 4°C. In a humidified chamber, primary antibodies diluted 1:50 in blocking buffer were added and incubated for 1 hour at 4°C, followed by three 10 minute rinses with blocking buffer. Secondary antibody (conjugated to Alexa Fluor 488) was added along with DAPI for 1 hour at room

temperature. Cells were then rinsed, and coverslips were mounted onto slides and then sealed. Cells were then imaged with a confocal microscope.

Immunoblotting

For assessment of Cav-1 expression, octyl-β-D-glucopyranoside (Millipore-Sigma; St. Louis, MO) was added at 60mM final concentration to RIPA buffer (Thermo Fisher Scientific; Waltham, MA) containing protease and phosphatase inhibitor cocktails (Roche; Basel, Switzerland). Protein concentration was determined with a *Dc* Protein Assay Kit (BioRad; Hercules, CA). For albumin immunoblots, 2 acid/salt washes with 0.1M glycine and 0.1M NaCl, pH 3.02 were performed on ice for 2 min each, followed by a PBS wash. Proteins were resolved by SDS/PAGE and transferred to nitrocellulose membranes. Membranes were incubated in 5% BSA in TBS-Tween blocking buffer for 1 hour at room temperature. Primary antibodies were allowed to bind overnight at 4°C, and used at a dilution of 1:500–1,000. After washing in TBS-Tween three times for 10 minutes each, the membranes were incubated with immunofluorescent secondary antibodies at a 1:5,000 dilution for 1 hour at room temperature. Membranes were washed with TBS-Tween prior to imaging via LI-COR Odyssey CLx Imaging System (Lincoln, NE).

Mass spectrometry

Mass spectrometry for determination of intracellular paclitaxel concentrations following NP treatment was performed as previously described (16). Briefly, NP (100 nM) or paclitaxel (100 nM)-treated and pre-treated gemcitabine (50 nM) samples in both AsPC-1 and HPAF-II cells were trypsinized, washed with cold PBS, and cell pellets were resuspended with 300 μL of 2:1 acetonitrile:water mixture. Metabolites were extracted by freeze-thawing the cell suspension in aqueous-acetonitrile (Aqu-ACN) followed by vortexing for 45 seconds. This procedure was repeated three times, and then centrifuging the contents at 13,000 rpm for 10 minutes at 4°C separated cell debris. The supernatants were separated from the debris and immediately the samples were analyzed in liquid chromatography mass spectrometry Triple Quad (LC-MS QQQ, Agilent 6430) instrument for quantitative assessment of paclitaxel in the intracellular compartment.

Cell Cycle Analysis

Following treatment, cells were trypsinized to generate single cell suspensions. Cells were pelleted at 500xG for 5 minutes and washed with PBS. Cells were pelleted again and resuspended in 400μL ice cold PBS. 800μL ice cold 100% ethanol was added drop-wise while mixing via vortexing on low, then incubated at 4°C overnight. Fixed cells were allowed to equilibrate to room temperature and gently resuspended by pipetting. Cells were pelleted at 500xG for 5 minutes and washed with PBS followed by pelleting again. Pellet was resuspended in 200μl propidium iodide (Roche; Basel, Switzerland) staining solution containing RNase (Millipore-Sigma; St. Louis, MO) and allowed to incubate for 30 minutes at 37°C protected from light. Cells were put on ice, still protected by light, and immediately taken to flow cytometer (BD FACSCalibur, BD Biosciences, San Jose CA) for analysis.

In vivo studies

Animal studies were conducted in accordance with an approved protocol adhering to the Institutional Animal Care and Use Committee policies and procedures at The Ohio State University (Columbus, OH). Six- to 8-week-old male athymic nude mice (Taconic Farms Inc.) were caged in groups of five or less, and fed a diet of animal chow and water ad libitum. AsPC-1, HPAF-II, and G37 cells were injected subcutaneously into the flanks of each mouse at 2×10^6 (AsPC-1 and HPAF-II) or 1×10^6 (G37) cells per injection. Treatment regimens were started once tumors reached approximately 100–200 mm^3 in size, 1–3 weeks post-injection. 20 mg/kg *nab*-paclitaxel in 0.9% saline was administered intravenously via retro-orbital injection, and 50 mg/kg gemcitabine in water was administered via intraperitoneal injection accordingly. To obtain a tumor growth curve, perpendicular diameter measurements of each tumor were measured every 1–5 days from the first day of injection with digital calipers, and volumes were calculated using the formula (L × W × W)/2. For ultrasound imaging of the pancreatic tumors following orthotopic injection of 1×10^4 of the G37 cells, we utilized our institutional Vevo 2100 ultrasound imaging system. Following anesthetization using isoflurane, mice were placed supine on the imaging platform. A MS200 transducer was placed on the ultrasound gel over the abdomen. Following identification of the pancreas, a 3D image was obtained using a 3D transducer setup of the entire abdomen starting superior at the diaphragm and ending inferior at the bladder. Tumors were identified on this 3D image and 2 measurements were recorded, length and depth. Volume was calculated on the formula $V = (4/3) \times \pi \times (L/2) \times (L/2) \times (D/2)$.

Statistical analysis

Data are presented as the mean ± SEM for proliferation assays, mass spectrometry data, and tumor growth experiments. The group comparisons of the percent change in tumor volume were performed at individual time points. Statistical comparisons were made between the control and experimental conditions using the unpaired two-tailed Student t test with significance assessed at $P < 0.05$. For the orthotopic *in vivo* study a one-tailed Student t test was used because our xenograft modeling showed better outcomes with altered sequencing vs normal sequencing. GraphPad Prism (GraphPad Software Inc.) was used to perform the statistical analyses.

RESULTS:

Gemcitabine treatment of PDAC cells increases Cav-1 expression, as well as albumin and NP uptake in vitro.

AsPC-1 ($KRAS^{G12D}$; $p53^{C135fs}$) and HPAF-II ($KRAS^{G12D}$; $p53^{P151S}$) PDAC cell lines have relatively low Cav-1 expression compared to other PDAC cell lines (13). We first tested whether gemcitabine could increase Cav-1 levels in AsPC-1 and HPAF-II cells. These two PDAC cells were treated for 8, 24, and 48 hours with gemcitabine (50 nM) followed by isolation of protein and RNA for analysis of Cav-1 expression. Similar to findings we observed in other PDAC cell lines (13), gemcitabine treatment for 48 hours resulted in a ~2-fold increase in both RNA and protein Cav-1 expression in AsPC-1 cells ($p<0.05$, Fig. 1A,C) and a 6- and 2-fold increase in RNA and protein expression, respectively, for HPAF-II

cells ($p<0.0001$, Fig. 1B,D). Similar results were also observed in the G37 cell line and the murine KPC-Luc pancreatic tumor derived cell line (Supplementary Figure 1, top). Next we tested whether gemcitabine treatment would increase albumin uptake in AsPC-1 and HPAF-II cells *in vitro*. Gemcitabine treatment of PDAC cells for 24 or 48 hours followed by a one hour pulse of HSA increased the amount of intracellular albumin detected via immunoblotting compared to the control-treated sample (HSA pulse without gemcitabine pre-treatment, Fig. 1E−F). Extended 7-day treatment of AsPC-1 and HPAF-II with gemcitabine demonstrated that Cav-1 expression was maintained over extended time periods (Fig. 1G). Next, we measured the albumin bound to paclitaxel in NP by immunofluorescence in both AsPC-1 and HPAF-II cells following a one hour pulse of NP (Fig. 2A−B). Pre-treatment with gemcitabine for 24 hours followed by a one hour NP pulse on day 2 or day 3 after gemcitabine treatment resulted in a significant increase in intracellular albumin signal compared to the untreated NP-treated control cells (Fig. 2A−D, $p<0.0001$). To directly quantify intracellular NP, we performed mass spectrometry analysis and measured uptake of paclitaxel in both AsPC-1 and HPAF-II cells. We found gemcitabine pre-treatment of 24 or 48 hours increased intracellular paclitaxel uptake in both PDAC cell lines treated with NP for one hour compared to NP alone and gemcitabine delivered concurrent with NP (Fig. 2E−F, Supplementary Figure 2). Taken together, these results suggest that gemcitabine pre-treatment for up to 48 hours results in increased Cav-1 expression, as well as albumin and NP uptake, leading to increased intracellular paclitaxel *in vitro*.

Gemcitabine treatment prior to NP increases the therapeutic efficacy of the drug combination in vitro.

Next, we tested whether treating PDAC cells *in vitro* with gemcitabine prior to NP could improve the therapeutic efficacy of the drug combination. We first determined the half maximal inhibitory concentration (IC_{50}) dose for gemcitabine in various PDAC cell lines (Supplementary Figure 1, bottom). We next compared the therapeutic efficacy for the current clinical standard of gemcitabine and NP delivered on the same day (Gem(D1)NP(D1)) against two altered schedules: (A) gemcitabine treatment on Day 1 for 24 hours, followed by replacement with media lacking gemcitabine but containing NP on Day 2 for 24 hours (Gem(D1)NP(D2)); or (B) gemcitabine treatment on Day 1 for 24 hours, followed by replacement with media lacking gemcitabine for 24 hours, followed by NP treatment on Day 3 for 24 hours (Gem(D1)NP(D3)). The IncuCyte and alamarBlue assays were utilized to assess tumor cell proliferation with different treatment regimens *in vitro*. There was a significant reduction in cell proliferation in both AsPC-1 and HPAF-II cells treated with any of the three combination gemcitabine and NP schedules as compared with the vehicle control (Fig. 3A−D). Both the Gem(D1)NP(D2) and Gem(D1)NP(D3) schedules resulted in significant reductions in growth rates in both the alamarBlue and IncuCyte assays compared to the Gem(D1)NP(D1) schedule (Fig. 3A−D, $P<0.01$). Additionally, Gem(D1)NP(D3) had a further significant reduction in cell proliferation compared to the Gem(D1)NP(D2) schedule after 72 hours in the alamarBlue assay (Fig. 3A−B, $P<0.01$). We next tested AsPC-1 and HPAF-II cells in the colony forming assay under different drug schedules. Survival was significantly reduced for both the Gem(D1)NP(D2) and Gem(D1)NP(D3) compared to Gem(D1)NP(D1) with 1 cycle of therapy (Fig. 3E−H). Additionally, tumor cell

survival was significantly reduced in the Gem(D1)NP(D3) schedule compared to Gem(D1)NP(D2) in both AsPC-1 and HPAF-II cell lines (Fig. 3E−H). These results were reproduced in the G37 and KPC cell lines (Supplementary Figure 3A−D). Furthermore, we performed extended time course colony formation assays with multiple “cycles” of the treatment regimens and similarly found that altered scheduling produced the most profound reductions in colony formation (Fig. 3E−H). Interestingly, we tested higher Cav-1 expressing PDAC cell lines (BxPC3, Panc-1, and CFPAC-1)with the altered scheduling regimen and found heterogeneity of response between the Gem(D1)NP(D1) and the Gem(D1)NP(D2) scheduling (Supplementary Figure 3E−G). Consistent with decreased cell survival noted with the Gem(D1)NP(D3) schedule, apoptotic markers such as cleaved PARP, cleaved caspase 8, 7, and 3 were all increased in the Gem(D1)NP(D3) schedule (Fig. 4A). We next tested if altering the schedule of the drug combination would impact normal cell growth. Normal small intestine FHs-74 Int cells were treated as described for the PDAC cells, and cell growth measured by the IncuCyte assay over 136 hours (Supplementary Figure 4). There were no observed significant differences in cell growth between any of the different chemotherapy treatment schedules.

Loss of Cav-1 leads to reduced albumin uptake and response to altered scheduling of gemcitabine and NP.

Next, to determine if Cav-1 expression is critical for the observed gemcitabine-induced albumin uptake, we performed stable knockdown of Cav-1 by shRNA (versus control scrambled shRNA) in a relatively high Cav-1 expressing cell line, MIA-PaCa-2 (MP2) (Fig. 4A). We confirmed that gemcitabine treatment for 24 hours increased both Cav-1 expression and albumin uptake in the control shRNA MP2 cells. However, in the Cav-1 depleted MP2 cells (shCav-1), there was less intracellular albumin uptake following gemcitabine treatment compared to the shRNA control cells (Fig. 4A). This result supports the important role of Cav-1 in gemcitabine induced albumin uptake. Next, to confirm that Cav-1 is partly responsible for the increased therapeutic efficacy of the altered scheduling *in vitro*, we performed colony formation again for the different schedules of gemcitabine and NP in both the MP2 sh-control and MP2 sh-Cav-1 cells. In the sh-control cells, Gem(D1)NP(D3) resulted in a significant reduction in survival compared to either the Gem(D1)NP(D1) or Gem(D1)NP(D2), similar to the results seen in the AsPC-1 and HPAF-II cells. However, in the sh-Cav-1 MP2 cells, the benefit of the altered scheduling of gemcitabine and NP was abrogated (Fig. 4B).

Cell cycle synchronizing effects of gemcitabine treatment contribute to the increased efficacy observed with altered scheduling of gemcitabine and NP.

The mechanism of action of paclitaxel is to stabilize microtubules during mitosis and prevent proper cell separation into two daughter cells.(10) Therefore, one strategy to optimize NP response might be to increase the proportion of cells in the G2/M phase of the cell cycle when paclitaxel is administered to tumor cells. We speculated that gemcitabine treatment could be altering distribution of PDAC cells in the cell cycle allowing for enhanced NP-mediated cell kill at 48 hrs after gemcitabine. To assess this, AsPC-1 and HPAF-II cells were treated with gemcitabine for 24 hours followed by exchange with media lacking gemcitabine for an additional 48 hours. Cells were fixed at 12 hour time points and

stained with propidium iodide for cell cycle analysis. We noted a reduction in the percentage of cells in the G2/M phase within the first 24–36 hours after gemcitabine treatment was initiated in both AsPC-1 and HPAF-II cells, likely due to intra-G1 and S phase arrest mechanisms (Fig. 5A). Interestingly, at 24–36 hours following the removal of gemcitabine, there was an observed “rush” of cells into the G2/M phase at 48–60 hours from treatment initiation (Fig. 5B−C), likely due to release of cells from G1 and S phase arrest. Taken together, it is possible that this progression of cells into G2/M at about the time that NP is administered is another mechanism that underlies the benefit of altered scheduling of gemcitabine and NP.

To further explore this hypothesis, we used drugs known to synchronize cells into either the G0/G1 or G2/M phases. First, we used the MEK inhibitor, trametinib, to arrest cells in the G0/G1 phase of the cell cycle. After 24 hours of trametinib treatment of AsPC-1 cells, the percentage of cells in the G0/G1 cell cycle phase increased from 57.3% to 92.9% (Fig. 5D). In colony forming assays, trametinib treatment for 24 hours resulted in no significant changes in clonogenic survival (Fig. 5E). Similarly, the addition of trametinib concurrently with NP on day 1 [Tram(D1)NP(D1)] did not alter the effectiveness of NP. However, when PDAC cells were pre-treated with trametinib for 24 hours prior to NP treatment [Tram(D1)NP(D2)], there was a marked reversal of the inhibition of clonogenic survival observed with either NP treatment alone or the combination trametinib and NP delivered on the same day (Fig. 5E). Similar results were obtained with HPAF-II cells (not shown). Bliss independence testing revealed trametinib to be antagonistic to NP, with a combination index (CI) score of 14.06 for the AsPC-1 cells and a CI of 2.14 for HPAF-II cells (Supplementary Figure 5A). We next tested the contrasting scenario by forcing cells into the G2/M phase of the cell cycle prior to NP treatment. AsPC-1 cells were treated with the drug RO-3306, a selective ATP-competitive inhibitor of the G2/M checkpoint regulator, CDK-1. This drug has been previously shown to induce G2/M cell cycle arrest (19). Following 24 hours of treatment with RO–3306 (10 μM), the percentage of cells in the G2/M phase increased from 19.1% to 66.8% as expected (Fig. 5F). In colony forming assays, RO-3306 treatment alone had no impact on survival, but concurrently treating [RO(D1)NP(D1)] or pre-treating with RO-3306 for 24 hours followed by NP on day 2 [RO(D1)NP(D2)] significantly reduced clonogenic survival compared to NP alone (Fig. 5G). In addition, RO(D1)NP(D2) demonstrated reduced tumor cell survival compared to concurrent treatment [RO(D1)NP(D1)]. Sequential treatment with RO(D1)NP(D2) was also determined to have a synergistic effect based on Bliss Independence testing with a CI of 0.67 (Supplementary Figure 5B). These cell cycle results provide an additional explanation for the increased efficacy of the altered gemcitabine and NP schedules.

Altered scheduling enhances the therapeutic efficacy of gemcitabine and nab-paclitaxel in murine models of PDAC

We next tested whether the altered scheduling of gemcitabine and NP could increase the therapeutic efficacy of the drug combination in subcutaneous (heterotopic) and orthotopic models of PDAC. Following tumor formation, mice were randomized to one of four treatment schedules delivered in 3 cycles over 9–11 days: (1) vehicle control, (2) gemcitabine alone, (3) Gem(D1)NP(D1), or (4) Gem(D1)NP(D3) (Supplementary Figure 6).

There were no significant differences in tumor volumes at baseline; however, by day 10 (AsPC-1 and HPAF-II) or day 5 (G37) post treatment initiation, there was a significant reduction in tumor volume in mice receiving the Gem(D1)NP(D3) regimen compared to Gem(D1)NP(D1) (Fig. 6A, C, E $p<0.001$). The tumor-doubling times in the Gem(D1)NP(D3) group compared to the Gem(D1)NP(D1) group were markedly longer (log rank $p<0.0001$) (Fig. 6 B, D, F $p<0.0001$). In terms of toxicities, there were no significant differences in weight loss between the groups or in clinical tolerance of the mice to the different scheduling regimens (Supplementary Fig. 7). We next tested the efficacy of the altered schedule of gemcitabine plus NP in an orthotopic murine model by injecting 1×10^4 G37 cells into the pancreata of athymic mice. One week post-injection the mice were randomized to (1) vehicle control, (2) Gem(D1)NP(D1), or (3) Gem(D1)NP(D3) treatment regimens as described in the xenograft model. Abdominal ultrasound imaging was utilized starting week 1 post-treatment course to measure tumor dimensions and volume *in vivo*. There was a significant reduction in tumor volumes at one and two weeks post treatment in both the Gem(D1)NP(D1) and Gem(D1)NP(D3) regimens compared to vehicle control group (Fig. 8A, $p<0.05$). Importantly, there was also a significant reduction in tumor volumes at one and three weeks post treatment in the Gem(D1)NP(D3) group compared to Gem(D1)NP(D1) group (Fig. 6G, $p<0.05$). We next injected 1×10^4 cells KPC-Luc (luciferase-bearing) cells into the pancreata of athymic mice, and randomized the mice into the 3 treatment groups one week later as described in the G37 orthotopic experiment. After 3 weeks, mice were sacrificed, and the ratio of pancreas to body weight was significantly reduced in both the Gem(D1)NP(D1) group ($p=0.05$) and the Gem(D1)NP(D3) group compared to the control mice ($p=0.01$) (Fig. 6H). The pancreas to body weight ratios in the Gem(D1)NP(D3) group compared to Gem(D1)NP(D1) were also significantly reduced, indicating increased efficacy with altered gemcitabine and NP scheduling ($p=0.05$).

DISCUSSION:

Nab-paclitaxel and gemcitabine combination therapy is now one of the preferred treatment options for advanced PDAC. NP (originally called ABI-007), an albumin-bound chemotherapy, was generated to overcome the poor solubility issues of the Cremophor-EL solvent required for free paclitaxel (20). Subsequent clinical trials showed that NP improved efficacy and toxicity profiles over standard paclitaxel in breast and non-small cell lung cancer trials (21, 22). Interestingly, minimal attention is often paid to optimizing treatment schedules of combinations of chemotherapy drugs prior to clinical testing. With this is mind, we tested alternative delivery schedules based on the current knowledge of albumin physiology and biology in tumor cells using preclinical models of PDAC and found marked improvements in efficacy with delaying administration of NP 24–48 hours after gemcitabine. Our findings appear to be related to increased expression of Cav-1 and cell cycle dependent effects of gemcitabine pre-treatment. If clinically validated, our results could lead to a new standard of care for patients receiving gemcitabine and *nab*-paclitaxel

Immunoprecipitation studies have shown membrane associated albumin-binding glycoprotein (gp60) associates with caveolin-1 after gp60 binding to albumin (35). Caveolae and thus Cav-1 are critical for the process of gp60 mediated albumin transcytosis (36). Caveolae are 50–100 nM flask-shaped invaginations of the plasma membrane that are

important for endocytosis and cholesterol homeostasis, and Cav-1, a scaffolding protein, is necessary for caveolae formation (12). Cav-1 has been found to be overexpressed in a variety of cancer types, including prostate, esophageal, non-small cell lung, breast, and pancreatic cancers ((37–42). Interestingly, Cav-1 has been shown to be either a tumor suppresser or tumor promoter depending on the cancer type (43). In the setting of PDAC, the majority of evidence supports Cav-1 as a tumor promoter, and Cav-1 has been previously shown to promote resistance to chemotherapy and radiation (13, 14, 44). In the large molecular subtyping classification studies by E. Collisson et al. as well as the TCGA publication, Cav-1 was associated with the more aggressive subtypes of PDAC, i.e. quasi-mesenchymal and basaloid subtypes (45, 46). Previous work from our lab showed Cav-1 is a critical mediator for NP uptake and the efficiency of NP was reduced following genetic knockdown of Cav-1 in pre-clinical PDAC models (16). There is recent evidence in other disease sites that Cav-1 expression correlates with NP response. In a single arm phase II clinical trial evaluating *nab*-paclitaxel and gemcitabine in 85 patients with metastatic breast cancer, both high tumor and stromal Cav-1 expression determined by immunohistochemistry (IHC) was associated with longer progression free survival (log rank p=0.03) (47). Additionally, for advanced non-small-cell lung cancer (NSCLC) a single arm phase II trial with carboplatin and *nab*-paclitaxel also showed high Cav-1 stromal expression by IHC was associated with both improved response rates and OS (48). Herein we show that loss of Cav-1 through RNA inhibition resulted in both reduced albumin uptake and lower sensitivity to NP and gemcitabine altered scheduling combinations (Fig. 4). Our data supports that gemcitabine mediated increases in Cav-1 over 24–48 hours facilitate increased uptake of NP, resulting in enhanced tumor cell kill.

Interestingly, our findings seemed to suggest that tumor cells with lower Cav-1 expression might be more effectively killed by altered scheduling (Figure 3 vs Supplemental Figure S3). AsPC-1, HPAFII, and G37 human pancreatic cancer cells that have low Cav-1 expression all significantly benefited from altered sequencing (Fig. 3, Supplementary Fig. S3), while higher Cav-1 expressing BxPC3 and CFPAC-1 cells demonstrated less tumor cell suppression (Supplemental Fig. S3). However, other moderate-high Cav-1 expressing cells lines Panc-1 (Supplemental Fig. S3) and MIA-PaCa2 (black bars on Fig. 4C), also seemed to benefit from altered scheduling. Taken together, our results suggest that in cells with higher baseline Cav-1, the effects of altered sequencing may be blunted, and that more study is warranted given the heterogeneity of response in higher Cav-1 expressing cell lines.

Another important finding in our study was that gemcitabine treatment resulted in synchronization of cells in the G0/G1 phase in the cell cycle at 24 hours, followed by a relatively synchronized enrichment of cells passing into G2/M phase 24–36 hours following gemcitabine removal (Fig. 4A−B). The ideal cell cycle phase for NP sensitization is the G2/M phase, due to the timing of microtubule separation. Thus, by treating cells with gemcitabine and NP concurrently, there might be less efficacy due to a greater proportion of cells arrested in the G0/G1 phase by gemcitabine, which could counteract the efficacy of NP, as supported by our finding of pre-treating cells with a G0/G1-arresting agent followed by NP (Fig. 5D). Similar evidence from Wang et al. demonstrated that cell synchronization into G0/G1 via thymidine block followed by fresh media exchange resulted in cells entering into

the G2/M phase, which likewise resulted in increased effectiveness of paclitaxel in ovarian cancer cell lines (49).

In summary, our data indicate that gemcitabine treatment increases Cav-1 expression and albumin uptake. Treating cells first with gemcitabine followed by NP at 48 hours was found to have the greatest inhibition of tumor cell growth both *in vitro* and *in vivo*. This strategy may be most useful in low Cav-1 expressing tumors, and thus Cav-1 might serve as a predictive biomarker for patients who would benefit most from sequential gemcitabine and nab-P/G treatment. As such, patients with low Cav-1 would stand to benefit most from sequential therapy, while patients with high Cav-1 would benefit less. Overall, our studies support further preclinical and clinical testing of altered scheduling of gemcitabine and NP for patients with PDAC, and represents a relatively simple and highly translatable novel treatment strategy that could result in dramatic improvements in treatment efficacy and a new standard of care with successful clinical validation.

Supplementary Material

Refer to Web version on PubMed Central for supplementary material.

ACKNOWLEDGMENTS

The content is solely the responsibility of the authors and does not necessarily represent the official views of the National Center for Advancing Translational Sciences or the National Institutes of Health. The authors thank M. Summers and M. Venere for use of IncuCyte system. The authors also thank the Analytical Cytometry and Small Animal Imaging Core (SAIC) at OSU for assistance with flow cytometry as well as *in vivo* ultrasound experiments.

Funding Support: This work was supported by the following grants: NIH R01 CA198128–01 (T.W.). Research reported in this article was also supported by The Ohio State University Comprehensive Cancer Center (OSU-CCC) and National Institute of Health (P30 CA016058).

REFERENCES

1. Siegel RL, Miller KD, and Jemal A. Cancer statistics, 2020. CA: A Cancer Journal for Clinicians. 2020;70(1):7–30. [PubMed: 31912902]
2. Rahib L, Smith BD, Aizenberg R, Rosenzweig AB, Fleshman JM, and Matrisian LM. Projecting Cancer Incidence and Deaths to 2030: The Unexpected Burden of Thyroid, Liver, and Pancreas Cancers in the United States. Cancer Research. 2014;74(11):2913–21. [PubMed: 24840647]
3. Katz MHG, Wang H, Fleming JB, Sun CC, Hwang RF, Wolff RA, et al. Long-Term Survival After Multidisciplinary Management of Resected Pancreatic Adenocarcinoma. Annals of Surgical Oncology. 2009;16(4):836. [PubMed: 19194760]
4. Burris HA 3rd, Moore MJ, Andersen J, Green MR, Rothenberg ML, Modiano MR, et al. Improvements in survival and clinical benefit with gemcitabine as first-line therapy for patients with advanced pancreas cancer: a randomized trial. J Clin Oncol. 1997;15(6):2403–13. [PubMed: 9196156]
5. Oettle H, Neuhaus P, Hochhaus A, Hartmann JT, Gellert K, Ridwelski K, et al. Adjuvant chemotherapy with gemcitabine and long-term outcomes among patients with resected pancreatic cancer: the CONKO-001 randomized trial. Jama. 2013;310(14):1473–81. [PubMed: 24104372]
6. Von Hoff DD, Ervin T, Arena FP, Chiorean EG, Infante J, Moore M, et al. Increased Survival in Pancreatic Cancer with nab-Paclitaxel plus Gemcitabine. New England Journal of Medicine. 2013;369(18):1691–703.
7. Conroy T, Desseigne F, Ychou M, Bouche O, Guimbaud R, Becouarn Y, et al. FOLFIRINOX versus gemcitabine for metastatic pancreatic cancer. N Engl J Med. 2011;364(19):1817–25. [PubMed: 21561347]

8. Conroy T, Hammel P, Hebbar M, Ben Abdelghani M, Wei AC, Raoul J-L, et al. FOLFIRINOX or Gemcitabine as Adjuvant Therapy for Pancreatic Cancer. New England Journal of Medicine. 2018;379(25):2395–406.

9. Mini E, Nobili S, Caciagli B, Landini I, and Mazzei T. Cellular pharmacology of gemcitabine. Annals of oncology : official journal of the European Society for Medical Oncology. 2006;17 Suppl 5:v7–12. [PubMed: 16807468]

10. Adams JD, Flora KP, Goldspiel BR, Wilson JW, Arbuck SG, and Finley R. Taxol: a history of pharmaceutical development and current pharmaceutical concerns. Journal of the National Cancer Institute Monographs. 1993(15):141–7. [PubMed: 7912520]

11. Desai N, Trieu V, Yao Z, Louie L, Ci S, Yang A, et al. Increased antitumor activity, intratumor paclitaxel concentrations, and endothelial cell transport of cremophor-free, albumin-bound paclitaxel, ABI-007, compared with cremophor-based paclitaxel. Clin Cancer Res. 2006;12(4):1317–24. [PubMed: 16489089]

12. Williams TM, and Lisanti MP. The Caveolin genes: from cell biology to medicine. Annals of medicine. 2004;36(8):584–95. [PubMed: 15768830]

13. Chatterjee M, Ben-Josef E, Thomas DG, Morgan MA, Zalupski MM, Khan G, et al. Caveolin-1 is Associated with Tumor Progression and Confers a Multi-Modality Resistance Phenotype in Pancreatic Cancer. Scientific Reports. 2015;5:10867. [PubMed: 26065715]

14. Suzuoki M, Miyamoto M, Kato K, Hiraoka K, Oshikiri T, Nakakubo Y, et al. Impact of caveolin-1 expression on prognosis of pancreatic ductal adenocarcinoma. British Journal of Cancer. 2002;87(10):1140–4. [PubMed: 12402154]

15. Witkiewicz AK, Nguyen KH, Dasgupta A, Kennedy EP, Yeo CJ, Lisanti MP, et al. Co-expression of fatty acid synthase and caveolin-1 in pancreatic ductal adenocarcinoma: implications for tumor progression and clinical outcome. Cell Cycle. 2008;7(19):3021–5. [PubMed: 18802406]

16. Chatterjee M, Ben-Josef E, Robb R, Vedaie M, Seum S, Thirumoorthy K, et al. Caveolae-Mediated Endocytosis Is Critical for Albumin Cellular Uptake and Response to Albumin-Bound Chemotherapy. Cancer Research. 2017;77(21):5925–37. [PubMed: 28923854]

17. Gomez-Chou SB, Swidnicka-Siergiejko AK, Badi N, Chavez-Tomar M, Lesinski GB, Bekaii-Saab T, et al. Lipocalin-2 Promotes Pancreatic Ductal Adenocarcinoma by Regulating Inflammation in the Tumor Microenvironment. Cancer Research. 2017;77(10):2647–60. [PubMed: 28249896]

18. Ma Y, Hwang RF, Logsdon CD, and Ullrich SE. Dynamic Mast Cell–Stromal Cell Interactions Promote Growth of Pancreatic Cancer. Cancer Research. 2013;73(13):3927–37. [PubMed: 23633481]

19. Vassilev LT. Cell Cycle Synchronization at the G2/M Phase Border by Reversible Inhibition of CDK1. Cell Cycle. 2006;5(22):2555–6. [PubMed: 17172841]

20. Desai N, Trieu V, Yao Z, Louie L, Ci S, Yang A, et al. Increased antitumor activity, intratumor paclitaxel concentrations, and endothelial cell transport of cremophor-free, albumin-bound paclitaxel, ABI-007, compared with cremophor-based paclitaxel. Clinical cancer research : an official journal of the American Association for Cancer Research. 2006;12(4):1317–24. [PubMed: 16489089]

21. Gradishar WJ, Tjulandin S, Davidson N, Shaw H, Desai N, Bhar P, et al. Phase III trial of nanoparticle albumin-bound paclitaxel compared with polyethylated castor oil-based paclitaxel in women with breast cancer. Journal of clinical oncology : official journal of the American Society of Clinical Oncology. 2005;23(31):7794–803. [PubMed: 16172456]

22. Socinski MA, Bondarenko I, Karaseva NA, Makhson AM, Vynnychenko I, Okamoto I, et al. Weekly nab-paclitaxel in combination with carboplatin versus solvent-based paclitaxel plus carboplatin as first-line therapy in patients with advanced non-small-cell lung cancer: final results of a phase III trial. Journal of clinical oncology : official journal of the American Society of Clinical Oncology. 2012;30(17):2055–62. [PubMed: 22547591]

23. Frese KK, Neesse A, Cook N, Bapiro TE, Lolkema MP, Jodrell DI, et al. nab-Paclitaxel potentiates gemcitabine activity by reducing cytidine deaminase levels in a mouse model of pancreatic cancer. Cancer Discov. 2012;2(3):260–9. [PubMed: 22585996]

24. Von Hoff DD, Ramanathan RK, Borad MJ, Laheru DA, Smith LS, Wood TE, et al. Gemcitabine Plus nab-Paclitaxel Is an Active Regimen in Patients With Advanced Pancreatic Cancer: A Phase I/II Trial. Journal of Clinical Oncology. 2011;29(34):4548–54. [PubMed: 21969517]
25. Peters T. All About Albumin: Biochemistry, Genetics, and Medical Applications. San Diego, CA 1996:Academic Press Limited.
26. Sleep D, Cameron J, and Evans LR. Albumin as a versatile platform for drug half-life extension. Biochimica et Biophysica Acta (BBA) - General Subjects. 2013;1830(12):5526–34. [PubMed: 23639804]
27. Tiruppathi C, Song W, Bergenfeldt M, Sass P, and Malik AB. Gp60 activation mediates albumin transcytosis in endothelial cells by tyrosine kinase-dependent pathway. The Journal of biological chemistry. 1997;272(41):25968–75. [PubMed: 9325331]
28. Commisso C, Davidson SM, Soydaner-Azeloglu RG, Parker SJ, Kamphorst JJ, Hackett S, et al. Macropinocytosis of protein is an amino acid supply route in Ras-transformed cells. Nature. 2013;497(7451):633–7. [PubMed: 23665962]
29. Schilling U, Friedrich EA, Sinn H, Schrenk HH, Clorius JH, and Maier-Borst W. Design of compounds having enhanced tumour uptake, using serum albumin as a carrier--Part II. In vivo studies. Int J Rad Appl Instrum B. 1992;19(6):685–95. [PubMed: 1522023]
30. Stehle G, Sinn H, Wunder A, Schrenk HH, Stewart JC, Hartung G, et al. Plasma protein (albumin) catabolism by the tumor itself--implications for tumor metabolism and the genesis of cachexia. Crit Rev Oncol Hematol. 1997;26(2):77–100. [PubMed: 9298326]
31. Carmeliet P, and Jain RK. Angiogenesis in cancer and other diseases. Nature. 2000;407(6801):249–57. [PubMed: 11001068]
32. Greish K. Enhanced permeability and retention of macromolecular drugs in solid tumors: a royal gate for targeted anticancer nanomedicines. J Drug Target. 2007;15(7–8):457–64. [PubMed: 17671892]
33. Schnitzer JE, and Oh P. Albondin-mediated capillary permeability to albumin. Differential role of receptors in endothelial transcytosis and endocytosis of native and modified albumins. Journal of Biological Chemistry. 1994;269(8):6072–82.
34. Von Hoff DD, Ramanathan RK, Borad MJ, Laheru DA, Smith LS, Wood TE, et al. Gemcitabine plus nab-paclitaxel is an active regimen in patients with advanced pancreatic cancer: a phase I/II trial. Journal of clinical oncology : official journal of the American Society of Clinical Oncology. 2011;29(34):4548–54. [PubMed: 21969517]
35. Minshall RD, Tiruppathi C, Vogel SM, Niles WD, Gilchrist A, Hamm HE, et al. Endothelial cell-surface gp60 activates vesicle formation and trafficking via G(i)-coupled Src kinase signaling pathway. J Cell Biol. 2000;150(5):1057–70. [PubMed: 10973995]
36. Schubert W, Frank PG, Razani B, Park DS, Chow CW, and Lisanti MP. Caveolae-deficient endothelial cells show defects in the uptake and transport of albumin in vivo. J Biol Chem. 2001;276(52):48619–22. [PubMed: 11689550]
37. Yang G, Truong LD, Wheeler TM, and Thompson TC. Caveolin-1 expression in clinically confined human prostate cancer: a novel prognostic marker. Cancer Res. 1999;59(22):5719–23. [PubMed: 10582690]
38. Kato K, Hida Y, Miyamoto M, Hashida H, Shinohara T, Itoh T, et al. Overexpression of caveolin-1 in esophageal squamous cell carcinoma correlates with lymph node metastasis and pathologic stage. Cancer. 2002;94(4):929–33. [PubMed: 11920460]
39. Yoo SH, Park YS, Kim HR, Sung SW, Kim JH, Shim YS, et al. Expression of caveolin-1 is associated with poor prognosis of patients with squamous cell carcinoma of the lung. Lung Cancer. 2003;42(2):195–202. [PubMed: 14568687]
40. Chen HL, Fan LF, Gao J, Ouyang JP, and Zhang YX. Differential expression and function of the caveolin-1 gene in non-small cell lung carcinoma. Oncol Rep. 2011;25(2):359–66. [PubMed: 21165568]
41. Sagara Y, Mimori K, Yoshinaga K, Tanaka F, Nishida K, Ohno S, et al. Clinical significance of Caveolin-1, Caveolin-2 and HER2/neu mRNA expression in human breast cancer. Br J Cancer. 2004;91(5):959–65. [PubMed: 15305200]

42. Tanase CP, Dima S, Mihai M, Raducan E, Nicolescu MI, Albulescu L, et al. Caveolin-1 overexpression correlates with tumour progression markers in pancreatic ductal adenocarcinoma. J Mol Histol. 2009;40(1):23–9. [PubMed: 19160064]

43. Williams TM, and Lisanti MP. Caveolin-1 in oncogenic transformation, cancer, and metastasis. American Journal of Physiology-Cell Physiology. 2005;288(3):C494–C506. [PubMed: 15692148]

44. Cordes N, Frick S, Brunner TB, Pilarsky C, Grützmann R, Sipos B, et al. Human pancreatic tumor cells are sensitized to ionizing radiation by knockdown of caveolin-1. Oncogene. 2007;26:6851. [PubMed: 17471232]

45. Collisson EA, Sadanandam A, Olson P, Gibb WJ, Truitt M, Gu S, et al. Subtypes of pancreatic ductal adenocarcinoma and their differing responses to therapy. Nat Med. 2011;17(4):500–3. [PubMed: 21460848]

46. Integrated Genomic Characterization of Pancreatic Ductal Adenocarcinoma. Cancer Cell. 2017;32(2):185–203.e13.

47. Zhao Y, Lv F, Chen S, Wang Z, Zhang J, Zhang S, et al. Caveolin-1 expression predicts efficacy of weekly nab-paclitaxel plus gemcitabine for metastatic breast cancer in the phase II clinical trial. BMC Cancer. 2018;18(1):1019. [PubMed: 30348118]

48. Bertino EM, Williams TM, Nana-Sinkam SP, Shilo K, Chatterjee M, Mo X, et al. Stromal Caveolin-1 Is Associated With Response and Survival in a Phase II Trial of nab-Paclitaxel With Carboplatin for Advanced NSCLC Patients. Clin Lung Cancer. 2015;16(6):466–74. [PubMed: 26123189]

49. Wang X, Pan L, Mao N, Sun L, Qin X, and Yin J. Cell-cycle synchronization reverses Taxol resistance of human ovarian cancer cell lines. Cancer Cell Int. 2013;13(1):77-. [PubMed: 23899403]

Translational Relevance:

Gemcitabine and albumin-bound paclitaxel (NP) combination chemotherapy delivered on the same day is now one of the preferred chemotherapy regimens for metastatic and locally-advanced pancreatic ductal adenocarcinoma (PDAC). Caveolin-1 (Cav-1), the principal structural component of caveolae and mediator of endocytosis, is highly expressed in PDAC cells and associated with enhanced tumor progression and resistance to gemcitabine in PDAC pre-clinical models. We found 24–48 hour gemcitabine treatment Cav-1 expression and subsequently increased albumin uptake, leading to maximal treatment efficacy with an optimized schedule of gemcitabine delivered on day 1 and NP on day 3 compared to the standard combination administered on the same day. These findings support further testing of an altered and biologically-optimized scheduling of gemcitabine and NP.

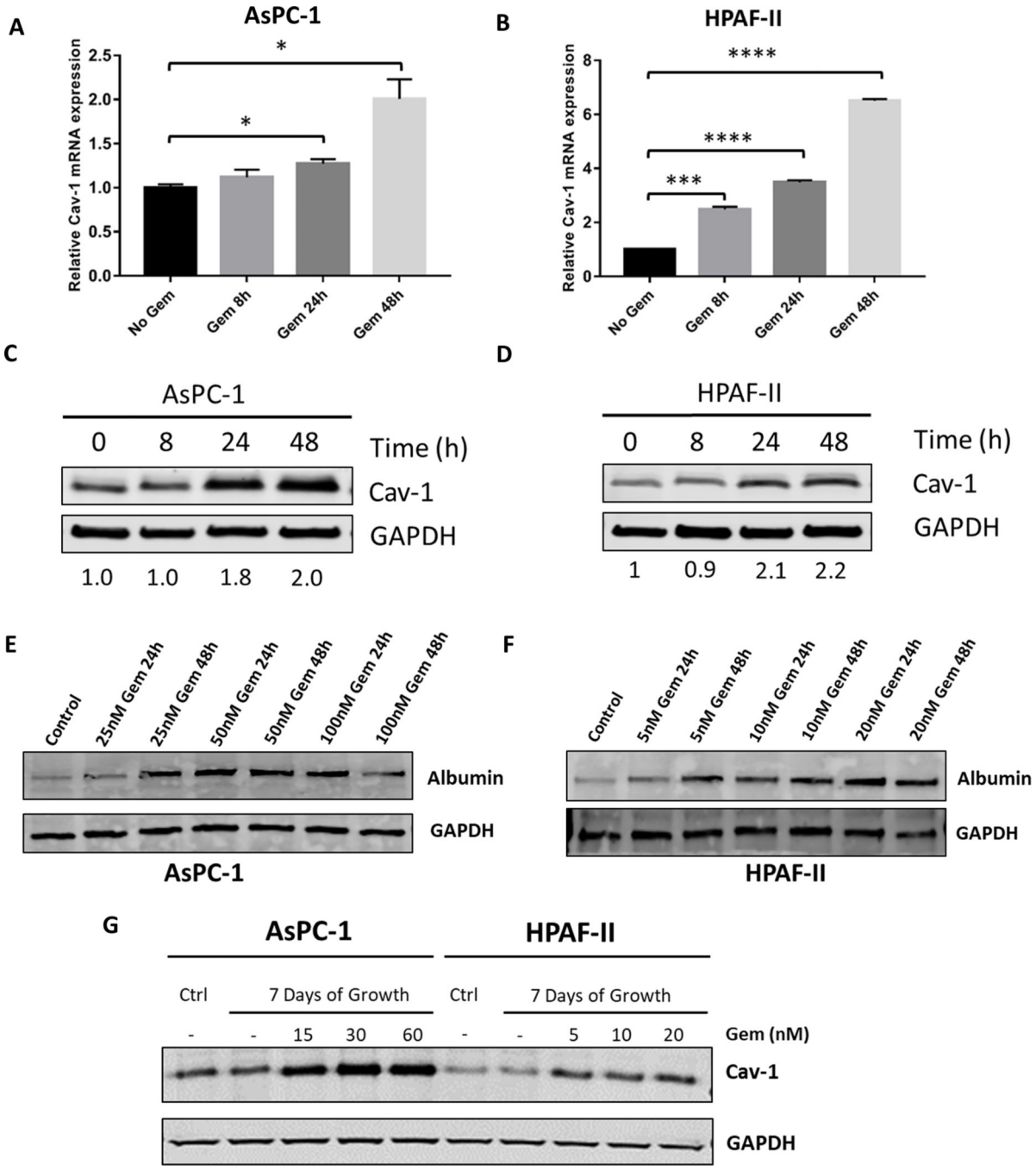

Figure. 1.

Gemcitabine treatment of PDAC cells increases Cav-1 expression and albumin uptake *in vitro*. **A-D**. AsPC-1 and HPAF-II cells were treated with gemcitabine (50 nM) for 8, 24, 48 hours and Cav-1 expression was measured by qRT-PCR (**A,B**) and western blot (**C,D**). Band quantitation with Image J software shown underneath (C,D). **E-F.** AsPC-1 and HPAF-II cells were treated with increasing doses of gemcitabine (25–100 nM for AsPC-1 and 5–20 nM for HPAF-II) for 24 hours or 48 hours followed by measurement of intracellular human albumin expression by western blot. **G.** Western blot of AsPC-1 and HPAF-II cells treated with

gemcitabine for 7 days at increasing gemcitabine concentrations compared to control (Ctrl) lysates made prior to treatment with 7 days of gemcitabine. *p < 0.05, **p < 0.01, ***p < 0.001, ****p<0.0001.

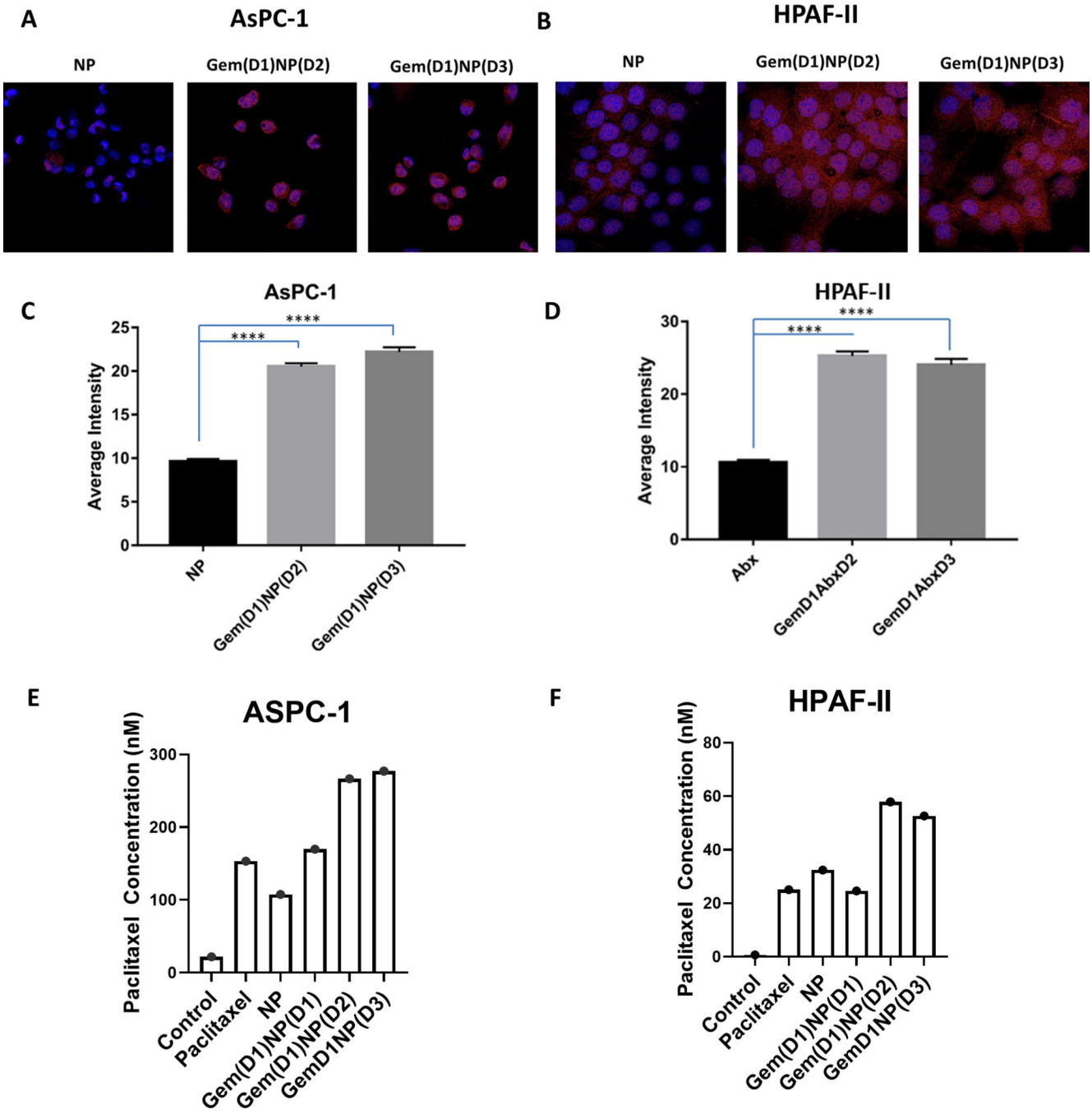

Figure. 2.

Gemcitabine pre-treatment of PDAC cells increases *nab*-paclitaxel uptake *in vitro* **A.** AsPC-1 and **B.** HPAF-II cells +/− pre-treatment with gemcitabine (50 nM) for 24 hours were pulsed with NP on day 2 (Gem(D1)NP(D2)) or day 3 (Gem(D1)NP(D3)) for one hour followed by immunofluorescence analysis of human albumin. Representative set of images of NP alone or cells pre-treated with gemcitabine for 24 hours are shown. **C-D.** Fluorescence intensity quantification was performed on Image J software based on raw integrated density of individual cells. **E-F**. Intracellular concentration of paclitaxel measured by mass

spectrometry was determined in ASPC-1 and HPAF-II cells after treatment with vehicle (control), paclitaxel (100 nM), or NP (100 nM) for one hour. In the last 3 conditions, gemcitabine (50 nM) was delivered concurrent [Gem(D1)NP(D1)], 24 hours [Gem(D1)NP(D2)] or 48 [Gem(D1)NP(D3)] hours prior to NP as indicated. ****$p<0.0001$.

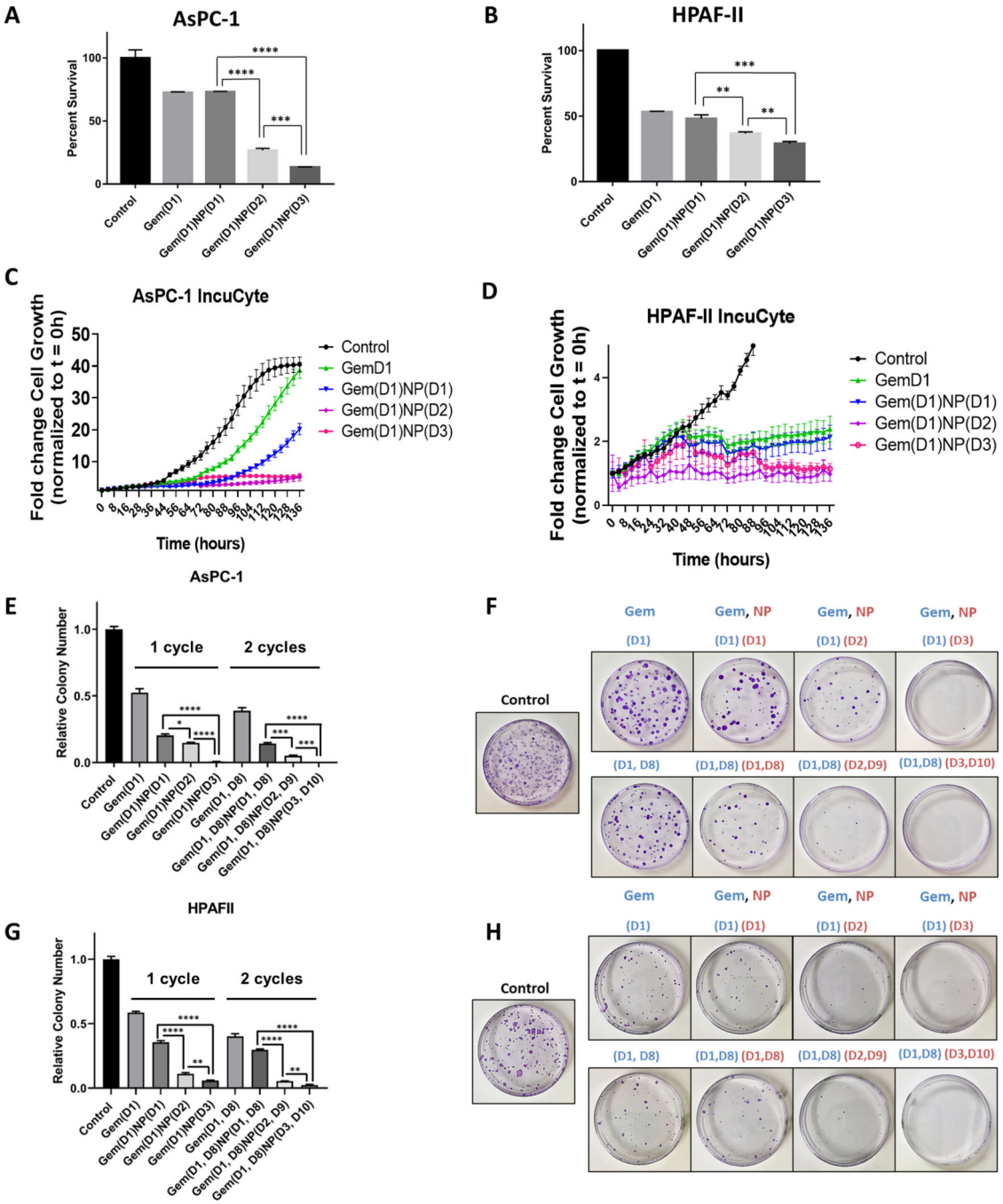

Figure 3.

Gemcitabine delivered prior to NP increases the therapeutic efficacy of the drug combination *in vitro*. **A-B.** AsPC-1 and HPAF-II cells were treated with vehicle control or gemcitabine (Gem, 50 nM) for a total of 24 hours with either NP (1 nM) delivered on same day [Gem(D1)NP(D1)], NP added on day 2 [Gem(D1)NP(D2)], or NP treated on day 3 with a 24 hour gap of no treatments [Gem(D1)NP(D3)]. NP and gemcitabine were removed after 24 hours of treatment for each condition. Following 72 hours from the start of treatments, proliferation was measured by the alamarBlue assay. Cell growth displayed as fold-change

from control condition (vehicle alone). **C-D**. AsPC-1 and HPAF-II cells tracked for 136 hours measuring confluence using the IncuCyte live-cell imaging system. Treatment schedules were kept the same as described in the alamarBlue assay (A-B). **E-H.** Extended time course colony forming assays (3 weeks) with corresponding plate images normalized to the control treatment (vehicle) are shown for AsPC-1 (E-F) and HPAF-II cells (G-H) for the different treatment schedules using 1 or 2 cycles of treatment. *p < 0.05, **p < 0.01, ***p < 0.001, ****p<0.0001.

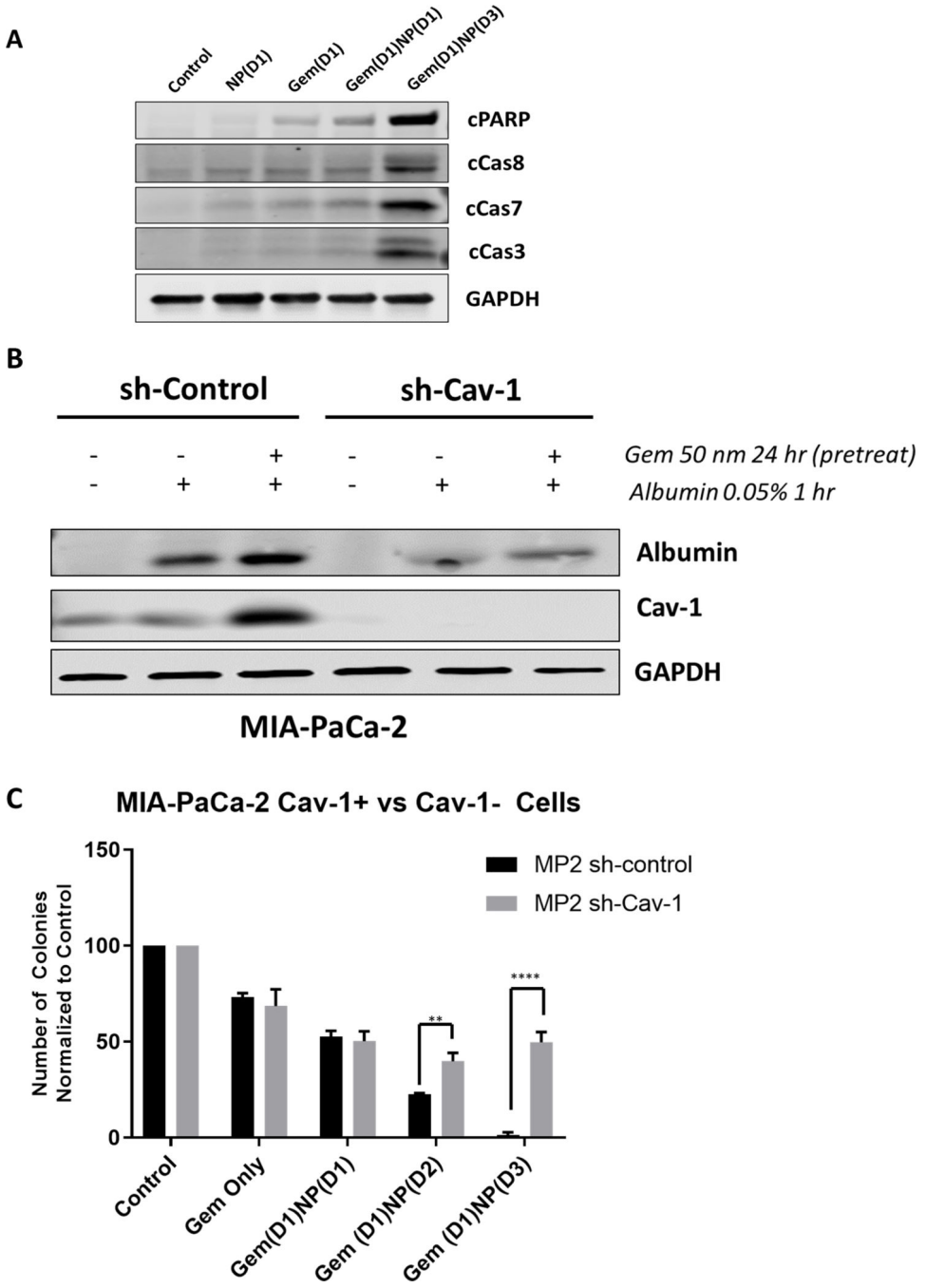

Figure 4.

Loss of Cav-1 leads to reduced albumin uptake and response to gemcitabine and NP. **A.** Western blot of apoptotic markers in AsPC-1 cells. Note that levels of cleaved PARP, cleaved caspase 8, 7, and 3 are highest in the Gem(D1)NP(D3) cells. Lysates were collected at 24 hours following start of last treatment. **B.** MIA-PaCa-2 control (scrambled shRNA) and shCav-1 (shRNA to Cav-1) stably transduced cells were treated with DMSO or gemcitabine (50 nM) for 24 hours followed by a pulse treatment of 0.05% weight/volume of human serum albumin (HSA) in cell culture medium for 1 hour prior to cell lysis. Loss of Cav-1

resulted in reduction in albumin uptake as measured by western blot with a HSA-specific primary antibody. **C.** Colony forming assays of MIA-PaCa-2 stable control and shCav-1 cells treated with either gemcitabine alone (50 nM), gemcitabine and NP (1 nM) treatment both on day 1 for 24 hours [Gem(D1)NP(D1)], gemcitabine on day 1 and NP on day 2 [Gem(D1)NP(D2)], or gemcitabine on day 1, no treatment on day 2, and NP on day 3 [Gem(D1)NP(D3)]. **p < 0.01, ****p<0.0001.

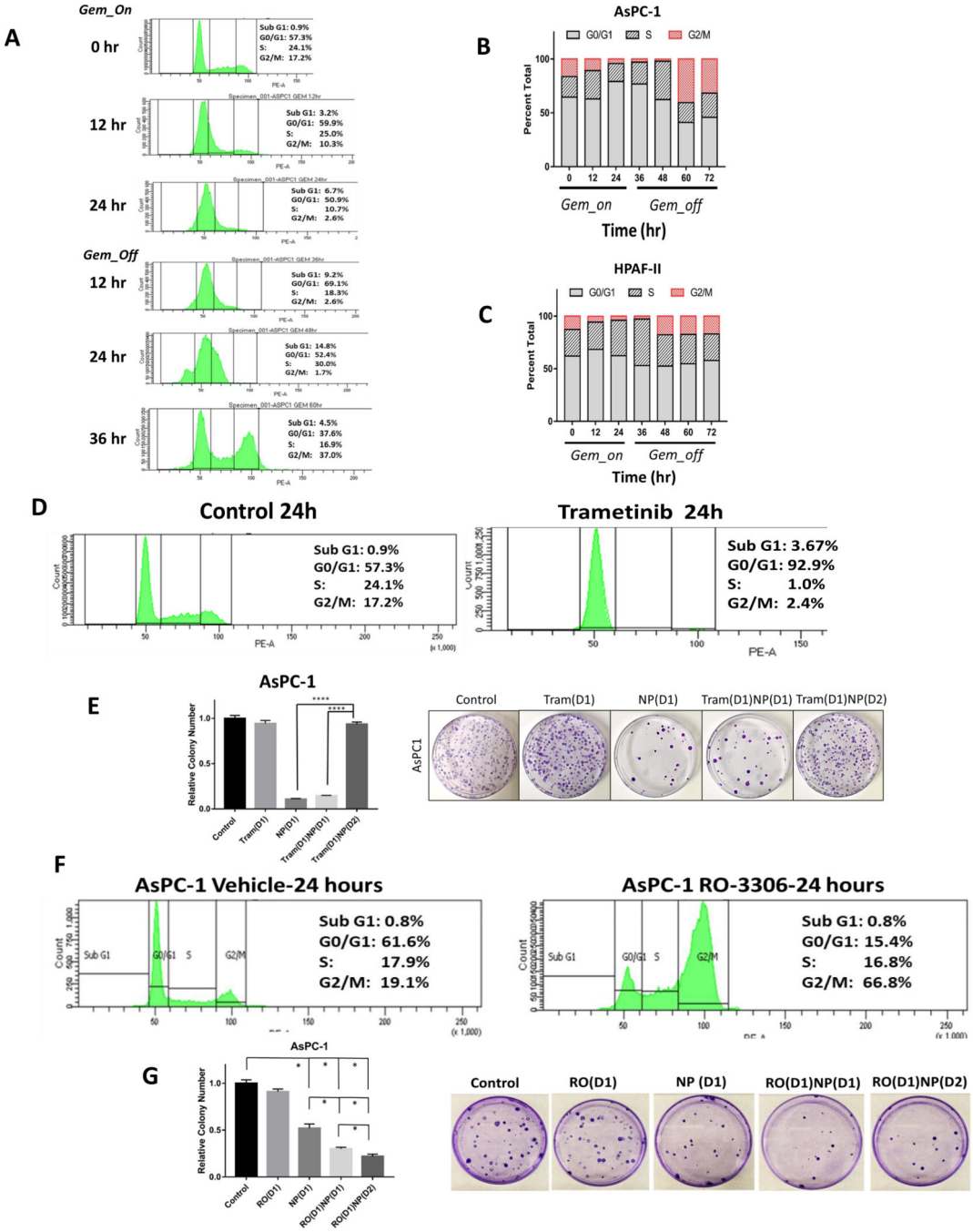

Figure 5.

Gemcitabine treatment results in cell cycle synchronization into G2/M phase after gemcitabine removal. **A.** Cell cycle analysis of AsPC-1 cells by propidium iodide staining following gemcitabine treatment (50 nM) for 24 hours and following removal of gemcitabine at 60 hours (36 hours after gemcitabine removal). **B**. Representative bar graphs of cell cycle percentages at 12 hour time points during gemcitabine treatment for AsPC-1 and **C**) HPAF-II cells shows increase of G2/M proportion after 24–36 hours after gemcitabine removal (at time 48–60 hr). **D.** Trametinib treatment for 24 hours arrests

AsPC-1 cells in the G0/G1 phase of the cell cycle. **E**. Pre-treatment of AsPC-1 cells with trametinib for 24 hours followed by 24 hour NP (1 nM) treatment [Tram(D1)NP(D2)] results in abrogation of colony forming inhibition observed with the treatment using NP alone or trametinib and NP treatment on the same day [Tram(D1)NP(D1)]. **F.** RO-3306 (10 μM) treatment for 24 hours arrests cells in the G2/GM phase of the cell cycle after staining with propidium iodide. **G.** Pre-treatment of AsPC-1 cells with RO-3306 for 24 hours, followed by NP treatment [RO(D1)NP(D2)] for 24 hours results in increased cell colony forming inhibition compared with RO-3306 alone [RO(D1)], NP alone [NP(D1)], or RO-3306 and NP treatment on the same day [RO(D1)NP(D1)]. *$p < 0.05$, **$p < 0.01$, ***$p < 0.001$, ****$p<0.0001$.

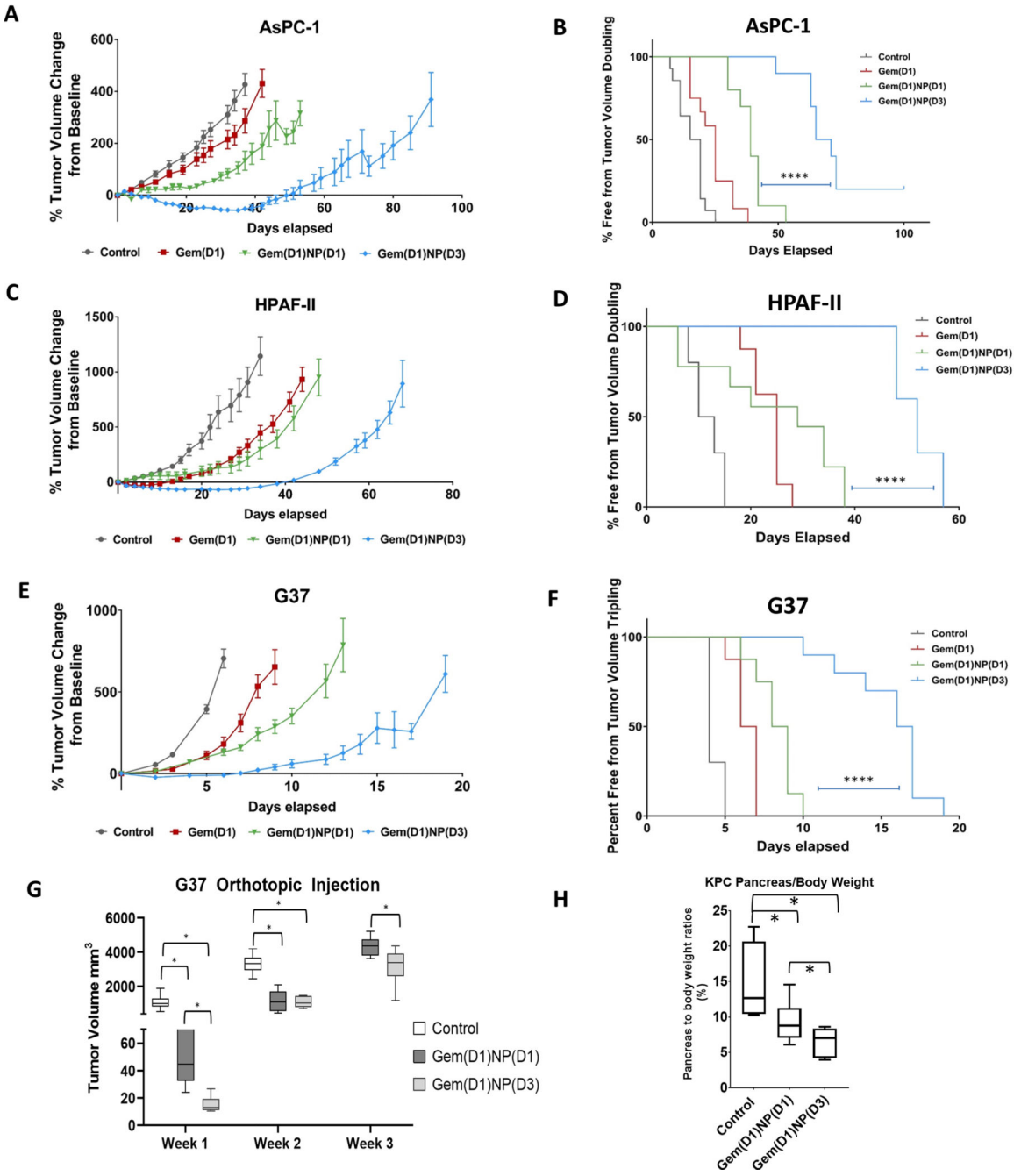

Figure 6.

Altered scheduling enhances the therapeutic efficacy of gemcitabine plus *nab*-paclitaxel in vivo. Tumor xenografts were formed by subcutaneously injecting 2.0×10^6 AsPC-1, HPAF-II, and 1.0×10^6 G37 cells into the flanks of athymic nude mice. Once tumors reached the initial starting volume (100–200 mm^3), mice were randomized to the 4 groups shown, with gemcitabine I.P. (50 mg/kg) always dosed on days 1,5,9 and NP I.V. (20 mg/kg) dosed on days 1,5,9 or 3,7,11. Tumor growth was measured up to 100 days. Tumor growth was significantly reduced in the Gem(D1)NP(D3) schedule compared to the concurrent

Gem(D1)NP(D1) schedule for **A**. AsPC-1, **C**. HPAF-II, and **E**. G37 cell lines. Tumor doubling time was significantly prolonged for the Gem(D1)NP(D3) schedule compared to the concurrent Gem(D1)NP(D1) schedule for **B**. AsPC-1, **D**. HPAF-II, and **F**. G37 cell lines. For each cell line, at least n=8–10 mice per study group were used. **G**. 1×10^4 G37 cells were implanted into the pancreata of athymic nude mice. One week post injection mice were randomized to three groups: control (saline), gemcitabine and NP delivered concurrently for 3 cycles on days 1,5,9 [Gem(D1)NP(D1)], or gemcitabine delivered on days 1,5,9 and NP on days 3,7,11 [Gem(D1)NP(D3]. Tumor volumes were measured starting one week following treatment conclusion by trans-abdominal ultrasound. **H.** KPC-Luc cells were injected into the pancreata of athymic nude mice and randomized one week post injection to the same treatment groups as described in the G37 orthotopic experiment. Pancreas to body ratios were recorded at the time of necropsy (n=4–6 mice per group). *p < 0.05, **p < 0.01, ***p < 0.001, ****p<0.0001.